RSC Advances

PAPER

View Article Online
View Journal | View Issue

Cite this: *RSC Adv.*, 2025, **15**, 6000

Alkyne dichotomy and hydrogen migration in binuclear cyclopentadienylmetal alkyne complexes†

Huidong Li,*[ab] Jinfeng Luo,[a] Haoyu Chen,[a] Ruilin Lu,[a] Yucheng Hu,[a] Huijie Wang,[a] Yanshu Wang,[a] Qunchao Fan,*[a] R. Bruce King *[b] and Henry F. Schaefer III [b]

The structures and energetics of the binuclear cyclopentadienylmetal alkyne systems $Cp_2M_2C_2R_2$ (M = Ni, Co, Fe; R = Me and NMe_2) have been investigated using density functional theory. For the $Cp_2M_2C_2(NMe_2)_2$ (M = Ni, Co, Fe) systems the relative energies of isomeric tetrahedrane Cp_2M_2(alkyne) structures having intact alkyne ligands and alkyne dichotomy structures $Cp_2M_2(CNMe_2)_2$ in which the C≡C triple bond of the alkyne has broken completely to give separate Me_2NC units depending on the central metal atoms. For the nickel system $Cp_2Ni_2C_2(NMe_2)_2$ as well as the related nickel systems $Cp_2Ni_2(MeC_2NMe_2)$ and $Cp_2Ni_2C_2Me_2$ the tetrahedrane structures are clearly preferred energetically consistent with the experimental syntheses of several stable Cp_2Ni_2(alkyne) complexes. The tetrahedrane and alkyne dichotomy structures have similar energies for the $Cp_2Co_2C_2(NMe_2)_2$ system whereas the alkyne dichotomy structures are significantly energetically preferred for the $Cp_2Fe_2C_2(NMe_2)_2$ system. The potential energy surfaces for the $Cp_2M_2(MeC_2NMe_2)$ and $Cp_2M_2C_2Me_2$ systems (M = Co, Fe) are complicated by low-energy structures in which hydrogen migration occurs from the alkyne methyl groups to one or both alkyne carbon atoms to give $Cp_2M_2(C_3H_3NMe_2)$ and $Cp_2M_2(C_3H_3Me)$ derivatives with bridging metalallylic ligands, $Cp_2M_2(CH_2{=}C{=}CHNMe_2)$ and $Cp_2M_2(CH_2{=}C{=}CHMe)$ with bridging allene ligands, as well as $Cp_2M_2(CH_2{=}CH{-}CNMe_2)$ and $Cp_2M_2(CH_2{=}CH{-}CHMe)$ with bridging vinylcarbene ligands. For the $Cp_2M_2C_2Me_2$ (M = Co, Fe) systems migration of a hydrogen atom from each methyl group to an alkyne carbon atom can give relatively low-energy $Cp_2M_2(CH_2{=}CH{-}CH{=}CH_2)$ structures with a bridging butadiene ligand. Five transition states have been identified in a proposed mechanism for the conversion of the Cp_2Co_2/MeC≡CNMe$_2$ system to the cobaltallylic complex $Cp_2Co_2(C_3H_3NMe_2)$ with intermediates having agostic C–H–Co interactions and an activation energy barrier sequence of 13.1, 17.0, 15.2, and 12.0 kcal mol^{-1}.

Received 23rd February 2024
Accepted 3rd January 2025

DOI: 10.1039/d4ra01410c

rsc.li/rsc-advances

1. Introduction

The chemistry of transition metal complexes with intact alkyne ligands originated with the 1956 discovery of cobalt carbonyl derivatives of the type (alkyne)$Co_2(CO)_6$, readily synthesized in good yield from reactions of alkynes with $Co_2(CO)_8$ under mild conditions[1–3] The structures of such (alkyne)$Co_2(CO)_6$ derivatives are characterized by a central Co_2C_2 tetrahedron having formal single bonds along each of the six edges of the central tetrahedron. In these structures the alkyne ligand donates four electrons to the central singly bonded Co_2 unit thereby giving each cobalt atom the favored 18-electron configuration (Fig. 1). The facile synthesis of (alkyne)$Co_2(CO)_6$ derivatives has led to extensive applications in synthetic organic chemistry[4,5] and catalysis.[6–9]

Reactions of iron carbonyls with alkynes typically require more vigorous conditions and lead to more complicated product mixtures. Dominant in such reaction mixtures are iron carbonyl complexes of ligands formed by the cyclization of two or three alkyne units including cyclobutadiene, cyclopentadienone, tropone, and ferracyclopentadiene (ferrole) ligands.[10] However, such alkyne oligomerizations are inhibited by bulky substituents. Thus among the products obtained from iron carbonyls

[a]*School of Science, Key Laboratory of High Performance Scientific Computation, Xihua University, Chengdu 610039, China*

[b]*Center for Computational Quantum Chemistry, University of Georgia, Athens, Georgia 30602, USA. E-mail: rbking@chem.uga.edu; huidongli@mail.xhu.edu.cn*

† Electronic supplementary information (ESI) available: Tables S1 to S11: Atomic coordinates of the optimized structures for the cmp-*n* (*n* = 1 to 6) and TS-*n* (*n* = 1 to 5) complexes in Fig. 15; Tables S12 to S22: harmonic vibrational frequencies (in cm^{-1}) and infrared intensities (in parentheses in km mol^{-1}) for the cmp-*n* (*n* = 1–6) and TS-*n* (*n* = 1–5) complexes in Fig. 15; Tables S23: the optimized structures of the cmp-*n* (*n* = 1–6) and TS-*n* (*n* = 1–5) complexes in Fig. 15; Tables S24 to S26: the optimized structures of the $Cp_2Ni_2C_2(NMe_2)_2$, $Cp_2Co_2C_2(NMe_2)_2$ and $Cp_2Fe_2C_2(NMe_2)_2$ complexes; Tables S27 to S29: the optimized structures of the $Cp_2Ni_2(MeC_2NMe_2)$, $Cp_2Co_2(MeC_2NMe_2)$ and $Cp_2Fe_2(MeC_2NMe_2)$ complexes; Tables S30 to S32: The optimized structures of the $Cp_2Ni_2C_2Me_2$, $Cp_2Co_2C_2Me_2$ and $Cp_2Fe_2C_2Me_2$ complexes. Separate .xyz file of the optimized structures. See DOI: https://doi.org/10.1039/d4ra01410c

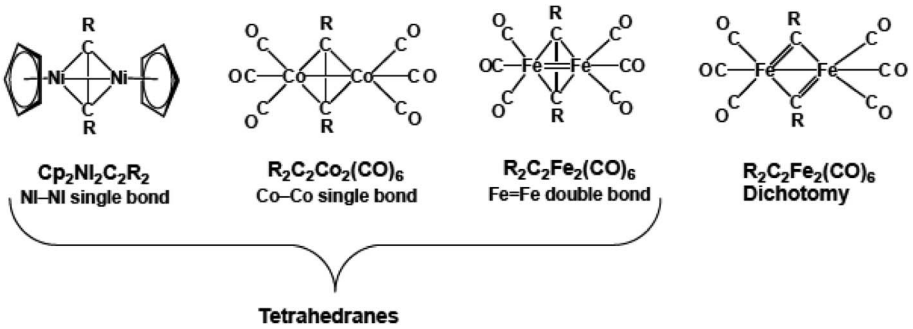

Fig. 1 Structures of some experimentally known alkyne metal complexes.

and di-*tert*-butylacetylene is *t*-$Bu_2C_2Fe_2(CO)_6$, shown by X-ray crystallography to have a central Fe_2C_2 tetrahedron similar to that in the (alkyne)$Co_2(CO)_6$ derivatives (Fig. 1).[11] The Fe=Fe distance of 2.316 Å in this Fe_2C_2 tetrahedron is ~0.13 Å shorter than the Co–Co single bond distance of 2.462 Å in the analogous *t*$Bu_2C_2Co_2(CO)_6$. This suggests the formal Fe=Fe double bond in *t*-$Bu_2C_2Fe_2(CO)_6$ required to give each iron atom the favored 18-electron configuration.

Alkyne oligomerization to give cyclic ligands in the iron carbonyl system can also be inhibited by dialkylamino substituents. Thus the reaction of $Et_2NC{\equiv}CNEt_2$ with iron carbonyls[12] was found to give a product of stoichiometry $(Et_2NC)_2Fe_2(CO)_6$ shown by X-ray crystallography to contain two separate Et_2NC diethylaminocarbyne units resulting from complete breaking of the C≡C triple bond in the original alkyne in a process known as dichotomy (Fig. 1).[13] Each Et_2NC unit contributes three electrons to the central Fe_2 unit so an Fe–Fe single bond in $(Et_2NC)_2Fe_2(CO)_6$ is sufficient to give each iron atom the favored 18-electron configuration. A density functional theory study has shown how dialkylamino substituents can favor alkyne dichotomy as compared with alkyl substituents without any donor atoms such as nitrogen.[14]

The robustness of the metal-cyclopentadienyl linkage makes CpM (Cp = η^5-C_5H_5) units good building blocks for transition metal complexes of diverse types that are likely to be more stable than their metal carbonyl counterparts. In this connection the CpNi unit is isoelectronic and isolobal with the $Co(CO)_3$ unit. Thus it is not surprising that several stable Cp_2Ni_2(alkyne) complexes have been synthesized by reactions of $Cp_2Ni_2(CO)_2$ with alkynes.[15–17] Similarly, the chemistry of Cp_2Co_2(alkyne) derivatives might be expected to parallel that of (alkyne)$Fe_2(CO)_6$ derivatives. However, Cp_2Co_2(alkyne) derivatives have not yet been synthesized since reactions of $CpCo(CO)_2$ with alkynes typically lead to alkyne cyclodimerization to give very stable CpCo(cyclobutadiene) derivatives or to alkyne cyclotrimerization to give benzene derivatives.[18]

Extending the isolobal analogy further suggests analogy between the chemistry of (alkyne)$Mn_2(CO)_6$ and Cp_2Fe_2(alkyne) derivatives. However, the alkyne chemistry of manganese carbonyl, which is of more recent origin than that of cobalt and iron carbonyls, follows a different pattern involving carbonyl richer systems. This reflects the need for each manganese atom to acquire two more ligand electrons than a cobalt atom to attain the favored 18-electron configuration. Thus the experimentally known diallkylaminoacetylene derivatives $(Et_2NC_2NEt_2)Mn_2(CO)_8$, $(Et_2NC_2Me)Mn_2(CO)_8$, and $(Me_2NC_2Ph)Mn_2(CO)_8$ are all examples of (alkyne)$Mn_2(CO)_8$ derivatives with central Mn_2C_2 tetrahedrane units analogous to the (alkyne)$Co_2(CO)_6$ derivatives but with one additional carbonyl group on each manganese atom.[12] This original work on alkyne manganese carbonyl chemistry focused on alkynes with dialkylamino substituents. Later the manganese carbonyl chemistry of alkynes with methyl substituents was found to be complicated by hydrogen migration from the methyl group to one or both alkyne carbon atoms to give species with bridging allene or manganallyl units (Fig. 2).[19]

We report here comprehensive density functional theory studies on Cp_2M_2(alkyne) (M = Ni, Co, Fe) systems with the three alkynes $Me_2NC{\equiv}CNMe_2$, $MeC{\equiv}CNMe_2$, and MeC≡CMe having the objective of guiding future experimental work in this area. In addition, our theoretical studies provide insight into hydrogen migration processes in alkyne metal carbonyl chemistry by suggesting a new mechanism for hydrogen migration in the $Cp_2Co_2(MeC_2NMe_2)$ system. The systems having dimethylamino substituents on the alkyne carbon atoms were chosen to

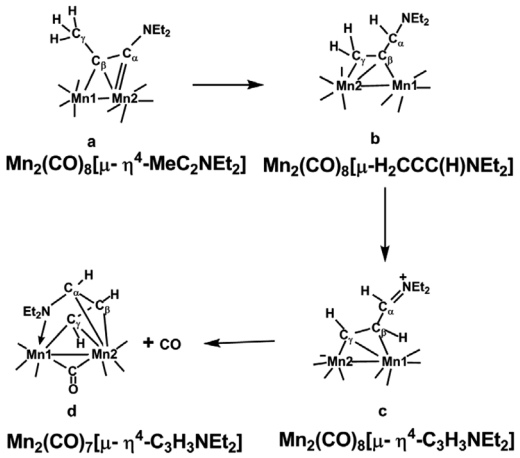

Fig. 2 Products formed by hydrogen migration from $Mn_2(CO)_8(MeC_2NEt_2)$ structurally characterized by X-ray crystallography.[19]

avoid the complication of possible hydrogen migration from methyl groups directly bonded to an alkyne carbon as observed experimentally for the manganese carbonyl derivatives.[19] The nickel derivatives Cp_2Ni_2(alkyne) are of interest both by being known experimentally[15–17] as well as by being analogues of the extensive series of (alkyne)$Co_2(CO)_6$ derivatives.[1–3] Analogy between the experimentally still unknown Cp_2Co_2(alkyne) systems and the (alkyne)$Fe_2(CO)_6$ systems suggest the possibility of alkyne dichotomy in low-energy Cp_2Co_2(alkyne) structures, particularly those with dialkylamino substituents.

2. Theoretical methods

The hybrid *meta*-GGA DFT methods M06-L[20,21] and ωB97xD[22] including empirical dispersion correction implemented in the Gaussian16 program,[23] were chosen for the calculations in order to consider possible agostic hydrogen and dispersion interactions. The B3PW91-D3 method[24] with Grimme's D3 dispersion[25] scheme was also used. These methods have been reported to give better overall performance for organometallic compounds than the first-generation functionals.[21,26] Double-ζ plus polarization (DZP) basis sets were used in conjunction with the M06-L method for the DFT optimizations. For carbon one set of pure spherical harmonic d functions with orbital exponent $\alpha_d(C) = 0.75$ was added to the standard Huzinaga–Dunning contracted DZ sets. This basis set is designated as (9s5p1d/4s2p1d).[27,28] For hydrogen, a set of *p* polarization functions $\alpha_p(H) = 0.75$ was added to the Huzinaga-Dunning DZ sets. For the first row transition metals the Wachters' primitive sets were used in our loosely contracted DZP basis sets, but augmented by two sets of *p* functions and one set of d functions, and contracted following Hood *et al.*, and designated as (14s11p6d/10s8p3d).[29,30] For testing the basis set effects on the geometry optimizations and electronic structures, the M06-L method with the def2-TZVP basis sets[31,32] was used to optimize fully the geometries based on the initial geometries predicted at the M06-L/DZP level. The results predicted at the higher level M06-L/def2-TZVP method are reported in the text. Other results based on the DZP basis sets are given in the ESI.†

The geometries of all structures were edited by hand starting from an XRD template and fully optimized by using the above DFT method with the (120, 974) integration grid. Small imaginary frequencies for the optimized structures were assumed to originate from numerical integration errors. Each structure is designated as ***m*N–M–*n*X**, where M is the symbol of the transition metal atom, m is the number of dimethylamino groups, n is the order of the structure in a sequence of increasing relative energies predicted by the M06-L/DZP method, and X designates the spin states, using S and T for singlets and triplets, respectively. The root-mean-square deviation (RMSD) value suggesting the structural difference of some singlet and triplet structural pairs were calculated by the RMSD code.[33] Only the energies predicted by the M06-L/DZP method and ωB97xD/DZP method are reported in the text. The distances (in Ångstroms) displayed in each figure are predicted by the M06-L/DZP method.

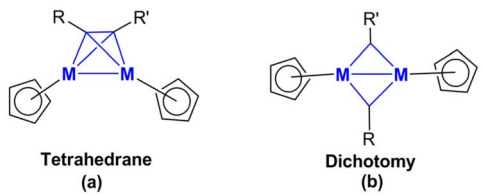

Fig. 3 The tetrahedrane and alkyne dichotomy structures for the $Cp_2M_2C_2RR'$ derivatives.

3. Results and discussion

3.1 Structures

3.1.1 $Cp_2M_2C_2(NMe_2)_2$. Two $Cp_2M_2C_2(NMe_2)_2$ (M = Fe, Co, Ni) structure types, namely the tetrahedrane structure and the dichotomy bis(carbyne) structure (Fig. 3), are found with their relative energies depending on the transition metal. Thus for the relatively electron-rich transition metal nickel (Fig. 4), the singlet tetrahedrane structure **2N–Ni–1S**, related to the experimentally known $Cp_2Ni_2(C_2R_2)$ derivatives,[15] lies much lower in energy than the alkyne dichotomy isomer **2N–Ni–4S** by 30.8 kcal mol^{-1}. The alkyne carbon–carbon distance of 1.366 Å in **2N–Ni–1S** is consistent with each of the orthogonal π-components of the C≡C triple bond donating an electron pair to one of the nickel atoms so that the alkyne ligand is a net four-electron donor to the central Ni_2 system. The predicted

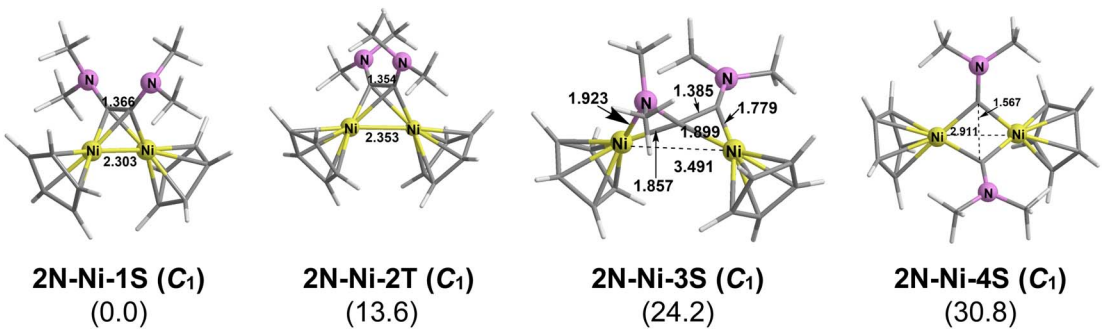

Fig. 4 The optimized low-energy $Cp_2Ni_2C_2(NMe_2)_2$ structures. The symmetry of the structure is indicated in parentheses in the first line. The numbers in parentheses in the second line are the relative emergies (Δ*E* in kcal mol^{-1}) predicted by M06-L/def2-TZVP method.

Ni–Ni distance of 2.303 in **2N–Ni–1S** can be interpreted as the Ni–Ni single bond required to give each nickel atom the favored 18-electron configuration. This Ni–Ni distance in **2N–Ni–1S** is very close to the experimental Ni–Ni distance of 2.33 Å in the diphenylacetylene complex $Cp_2Ni_2C_2Ph_2$ as determined by X-ray crystallography.[34] Structure **2N–Ni–1S** is the analogue of the well-known (alkyne)$Co_2(CO)_6$ derivatives[1–3] in which each $Co(CO)_3$ unit has been replaced with an isoelectronic CpNi unit.

The next higher energy $Cp_2Ni_2C_2(NMe_2)_2$ structure **2N–Ni–2T**, lying 13.6 kcal mol^{-1} above **2N–Ni–1S**, appears to be a triplet excited state of **2N–Ni–1S** (Fig. 4). The increase in the Ni–Ni distance in going from 2.303 Å in the singlet **2N–Ni–1S** to 2.353 Å in the corresponding triplet **2N–Ni–2T** is surprisingly small. The root-mean-square deviation (RMSD) was predicted to be 0.254 Å between the singlet **2N–Ni–1S** and the triplet **2N–Ni–2T**.

The $Cp_2Ni_2C_2(NMe_2)_2$ structure **2N–Ni–3S**, lying 24.2 kcal mol^{-1} above the lowest energy structure **2N–Ni–1S**, has a different coordination environment. In **2N–Ni–3S** one nickel atom is bonded to both alkyne carbon atoms with nickel-carbon distances of 1.899 Å and 1.779 Å corresponding to formal Ni–C single and Ni=C double bonds, respectively. The other nickel atom is connected to only one alkyne carbon atom with a Ni–C distance of 1.857 Å corresponding to a formal single bond but also to a nitrogen atom through a dative N→Ni bond of length 1.923 Å. The long Ni···Ni distance of 3.491 Å in **2N–Ni–3S** indicates the lack of a nickel–nickel bond. However, since each nickel atom receives three electrons from the alkyne ligand, each nickel atom has the favored 18-electron configuration.

The $Cp_2Ni_2C_2(NMe_2)_2$ structure **2N–Ni–4S** is a different type of dichotomy structure, with two separate three-electron donor Me_2NC dimethylaminocarbyne units bridging the nickel atoms with the carbyne carbon atom of such unit forming a Ni–C bond to each nickel atom (Fig. 4). Thus **2N–Ni–4S** has similar stereochemistry of the central Ni_2C_2 unit to that of the central Fe_2C_2 unit in the experimental $(Et_2NC)_2Fe_2(CO)_6$ dichotomy structure (Fig. 1)[13] except for a relatively long Ni···Ni distance of 2.911 Å suggesting the absence of a direct nickel–nickel bond. This is consistent with the 18-electron configuration of each nickel atom in a dimethylaminocarbyne structure $Cp_2Ni_2(CNMe_2)_2$ without a direct nickel–nickel bond.

For the cobalt system $Cp_2Co_2C_2(NMe_2)_2$ the tetrahedrane and dichotomy structures are spaced very close in energy with the dichotomy structure **2N–Co–1S** lying only 2.6 kcal mol^{-1} and 1.9 kcal mol^{-1} below the singlet and triplet tetrahedrane structures **2N–Co–3S** and **2N–Co–2T**, respectively (Fig. 5). In the dichotomy structure **2N–Co–1S** each of the separate bridging Me_2NC carbyne units donates three electrons to the central Co_2 unit. The Co–Co distance in **2N–Co–1S** of 2.351 Å suggests the formal single bond required to give each cobalt atom the

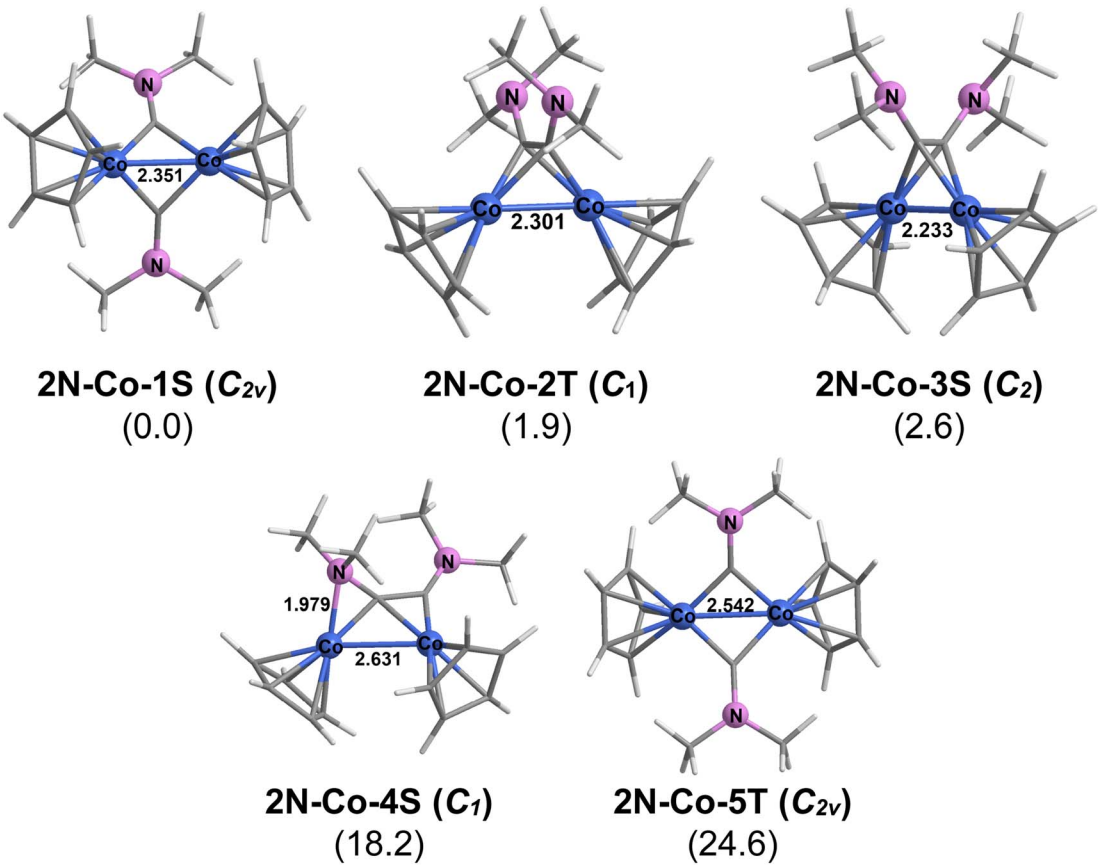

Fig. 5 The optimized low-energy $Cp_2Co_2C_2(NMe_2)_2$ structures. The symmetry of the structure is indicated in parentheses in the first line. The numbers in parentheses in the second are the relative energies (ΔE in kcal mol^{-1}) predicted by M06-L/def2-TZVP method.

favored 18-electron configuration. Structure **2N–Co–1S** is thus the analogue of the experimentally known and structurally characterized $(Et_2NC)_2Fe_2(CO)_6$ (Fig. 1)[11] in which each $Fe(CO)_3$ unit has been replaced by an isoelectronic CpCo unit. The Co═Co distance of 2.233 Å in the singlet tetrahedrane structure **2N–Co–3S** is ~0.1 Å shorter than the Co–Co distance in the dichotomy structure **2N–Co–1S** as well as the Ni–Ni single bond distance in the tetrahedrane structure **2N–Ni–1S**. Interpretation of the Co═Co distance in **2N–Co–3S** as a formal double bond gives each cobalt atom the favored 18-electron configuration. Thus **2N–Co–3S** is thus an analogue of the experimentally known iron tetrahedrane complex[11] $(tBu_2C_2)Fe_2(CO)_6$ in which each $Fe(CO)_3$ unit has been replaced by an isoelectronic CpCo unit. The Co═Co distance of 2.301 Å in the triplet tetrahedrane structure **2N–Co–2T** is essentially identical to that in the singlet analogue **2N–Co–3S** and thus can likewise be interpreted as a double bond thereby giving each cobalt the favored 18-electron configuration as in **2N–Co–3S**. The root-mean-square deviation (RMSD) was predicted to be 0.235 Å between the singlet **2N–Co–3S** and the triplet **2N–Co–2T**. The Co═Co double bond in the triplet **2N–Co–2T** is of the σ + 2/2 π type with two orthogonal one-electron π-components similar to the Fe═Fe double bond in the triplet state organometallic[35] $Cp_2Fe_2(\mu\text{-}CO)_3$ or normal dioxygen. The two singlet isomers **2N–Co–1s** and **2N–Co–3S** can interchange mutually by overcoming a very low activation energy barrier of ~6.0 kcal mol^{-1} (Fig. 6).

Two higher energy $Cp_2Co_2C_2(NMe_2)_2$ structures are of interest (Fig. 5). The singlet structure **2N–Co–4S**, lying 18.2 kcal mol^{-1} in energy above **2N–Co–1S**, has an intact $Me_2NC{\equiv}CNMe_2$ ligand functioning as a six-electron donor by bonding to the central Co_2 unit through both π-components of its C≡C triple bond as well as through an N→Co dative bond of length 1.979 Å from one of the amino nitrogen atoms. The Co–Co distance of 2.631 Å in **2N–Co–4S** is 0.3 to 0.4 Å longer than those in three lower energy $Cp_2Co_2C_2(NMe_2)_2$ isomers in Fig. 5 and thus can be interpreted as a formal single bond. Such a Co–Co single bond is sufficient to give each cobalt atom in **2N–Co–4S** the favored 18-electron configuration with a six-electron rather than four-electron donor bridging alkyne ligand. The other higher energy $Cp_2Co_2C_2(NMe_2)_2$ structure **2N–Co–5T**, lying 24.6 kcal mol^{-1} in energy above **2N–Co–1s**, is a triplet dichotomy structure related to the singlet dichotomy structure **2N–Co–1s** but with a significantly longer Co–Co distance of 2.542 Å. The root-mean-square deviation (RMSD) was predicted to be 0.651 Å between the singlet **2N–Co–1s** and the triplet **2N–Co–5T**. The triplet spin state of **2N–Co–5T** suggests that the two cobalt atoms are squeezed to a normally bonding distance by the geometry of the two bridging dimethylaminocarbyne ligands but are not able to form a bond instead retaining an unpaired electron on each cobalt atom.

The iron system $Cp_2Fe_2C_2(NMe_2)_2$ is the reverse of the nickel system since both the singlet and triplet dichotomy structures, **2N–Fe–1S** and **2N–Fe–2T**, respectively, are the lowest energy structures by substantial margins greater than 11 kcal mol^{-1} (Fig. 7). The root-mean-square deviation (RMSD) was predicted to be 0.255 Å between **2N–Fe–1S** and **2N–Fe–2T**. The Fe═Fe distance of 2.335 Å in **2N–Fe–1S** and 2.350 Å in **2N–Fe–2T** both can be considered as the formal double bonds required to give each iron atom the favored 18-electron configuration. In the singlet **2N–Fe–1S** the Fe═Fe double bond is of the normal σ + π type similar to that in ethylene. However, in the triplet **2N–Fe–2T** the Fe═Fe double bond is of the σ + 2/2π type similar to that in the organometallic[35] $Cp_2Fe_2(\mu\text{-}CO)_3$ or dioxygen.

The higher energy $Cp_2Fe_2C_2(NMe_2)_2$ structure **2N–Fe–3S**, lying 13.3 kcal mol^{-1} above **2N–Fe–1S**, has a tetrahedrane-like geometry but with a relatively long C–C distance of 1.691 Å suggesting a very weak interaction and a relatively short iron–iron distance of 2.268 Å approaching a formal triple bond. These C–C and Fe≡Fe distances suggest a resonance hybrid between a tetrahedrane and a dichotomy structure with both canonical forms having the favored 18-electron configuration for each iron atom.

The remaining two high-energy $Cp_2Fe_2C_2(NMe_2)_2$ structures, namely **2N–Fe–4T** and **2N–Fe–5S** lying 15.2 and 17.6 kcal mol^{-1} above **2N–Fe–1S**, respectively, each have a six-electron donor alkyne ligand using both π-components of the C≡C bond as well as a nitrogen lone pair through a dative N→Fe bond similar to the alkyne ligand in

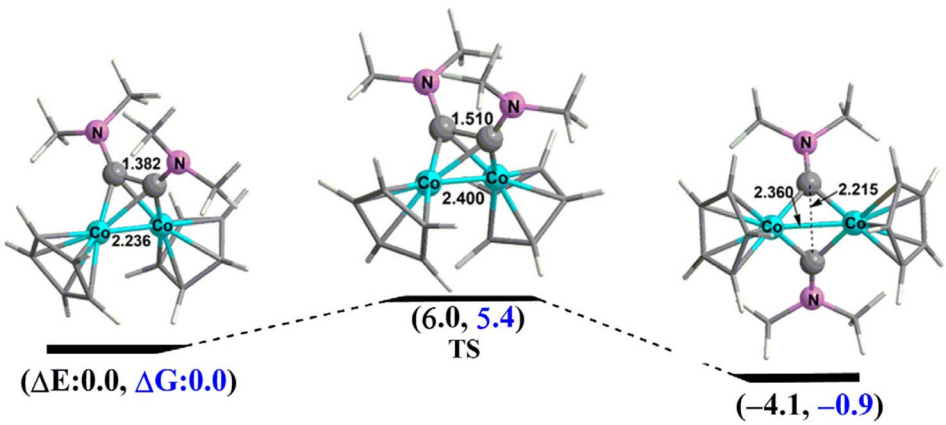

Fig. 6 The reaction pathway between the singlet tetrahedrane and dichotomy $Cp_2Co_2C_2(NMe_2)_2$ isomers **2N–Co–3S** and **2N–Co–1s**, respectively, showing the low energy barrier of ~6.0 kcal mol^{-1}. The numbers in parentheses are the relative energies predicted by M06-L/def2-TZVP method.

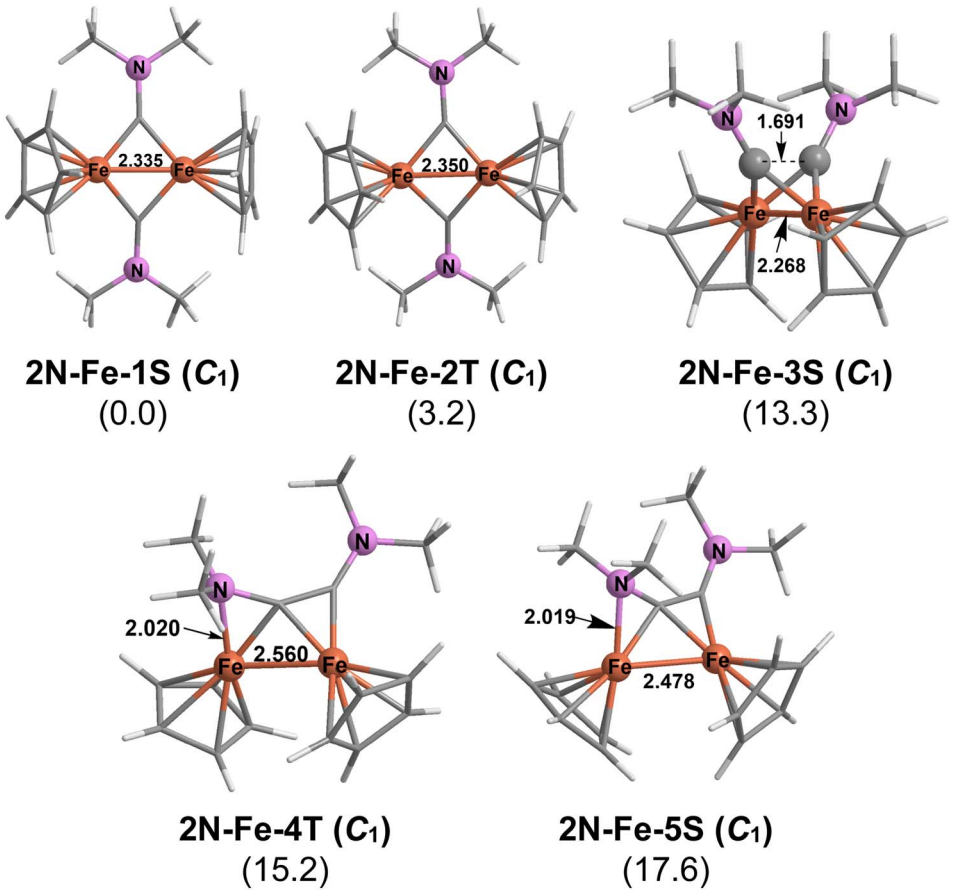

Fig. 7 The optimized low-energy $Cp_2Fe_2C_2(NMe_2)_2$ structures. The symmetry of the structure is indicated in parentheses in the first line. The numbers in parentheses in the second line are the relative energies (ΔE in kcal mol^{-1}) predicted by M06-L/def2-TZVP method.

2N–Co–4S (Fig. 7). Interpreting the 2.560 Å Fe–Fe distance in the triplet structure **2N–Fe–4T** as a formal single bond gives each iron atom a 17-electron configuration consistent with a binuclear triplet. The 2.478 Å of Fe=Fe distance in the singlet **2N–Fe–5S** is ~0.1 Å shorter than that in the otherwise similar **2N–Fe–4T** and thus can be interpreted as the formal

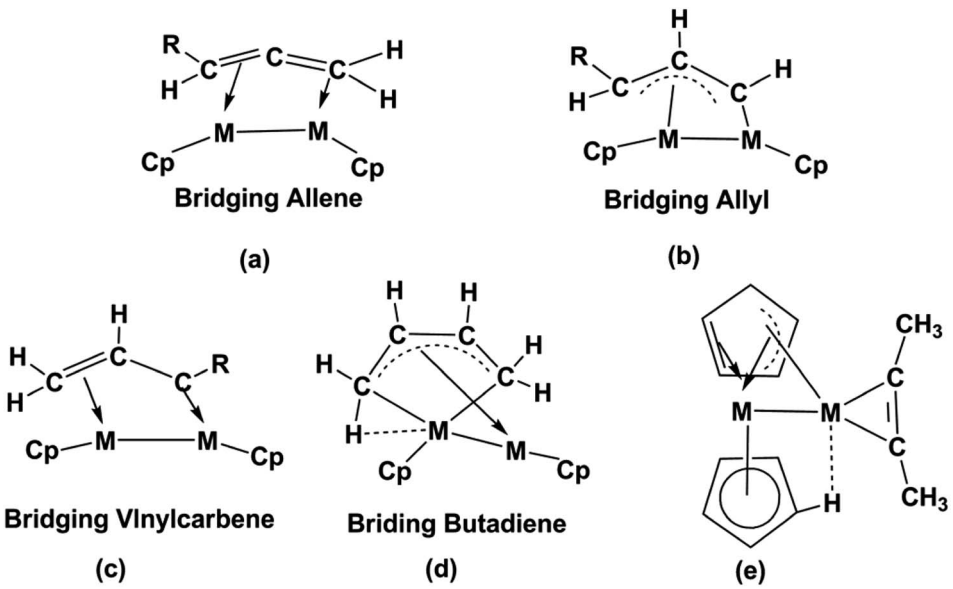

Fig. 8 Structure types formed by hydrogen migration from methyl groups in methylalkynes (a to d); an observed sandwich-type structure (e).

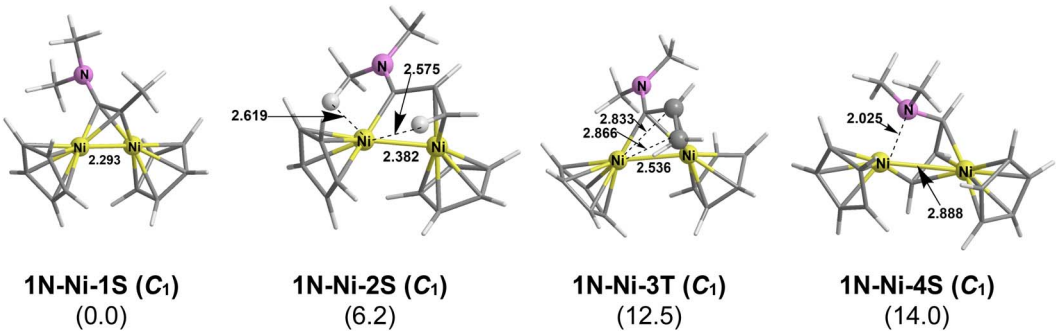

Fig. 9 The optimized low-energy $Cp_2Ni_2(MeC_2NMe_2)$ structures. The symmetry of the structure is indicated in parentheses in the first line. The numbers in parentheses in the second line are the relative energies (ΔE in kcal mol^{-1}) predicted by M06-L/def2-TZVP method.

double bond required to give each iron atom the favored 18-electron configuration.

3.1.2 $Cp_2M_2(MeC_2NMe_2)$ structures. The dimethylamino substituents in the $Cp_2M_2C_2(NMe_2)_2$ (M = Ni, Co, Fe) structures discussed above remain intact in all of the structures. Thus all of these structures have either intact $Me_2NC{\equiv}CNMe_2$ alkyne ligands or Me_2NC carbyne ligands formed by complete rupture of the alkyne C≡C triple bond. The potential surfaces become considerably more complicated when one or both of the dimethylamino substituents on the alkyne are replaced by methyl substituents. Hydrogen migration from such methyl substituents to one or both alkyne carbon atoms can lead to structures with bridging allene, metalallylic, or vinylcarbene ligands (Fig. 8). The first two structure types have been observed experimentally by Adams and coworkers in binuclear manganese carbonyl complexes of the $MeC{\equiv}CNEt_2$ ligand.[19]

Consider first binuclear cyclopentadienylmetal complexes of the type $Cp_2M_2(MeC_2NMe_2)$ (M = Ni, Co, Fe) having one methyl substituent on the alkyne ligand to provide a source of hydrogen atoms for migration to one or both alkyne carbon atoms (Fig. 8). Such hydrogen migration reactions can lead to complexes having bridging dimethylamino four-electron donor vinylcarbene ($CH_2{=}CH{-}CNMe_2$) ligands, four-electron donor metalallylic ligands ($C_3H_3NMe_2$), and four-electron donor allene ligands ($CH_2{=}C{=}CHNMe_2$). For the nickel system $Cp_2Ni_2(MeC_2NMe_2)$ the tetrahedrane structure **1N–Ni–1S** having an intact alkyne ligand with no hydrogen migration remains the lowest energy structure with an Ni–Ni distance of 2.293 Å (Fig. 9) that is close to the Ni–Ni distance of 2.303 Å in the $Cp_2Ni_2C_2(NMe_2)_2$ structure **2N–Ni–1S** discussed above (Fig. 4). However, **1N–Ni–2S** with a bridging four-electron donor vinylcarbene ligand formed by a single hydrogen migration and a Ni–Ni single bond distance of 2.382 Å lies only 9.2 kcal mol^{-1} in energy above **1N–Ni–1S**. A triplet version of the vinylcarbene complex, namely **1N–Ni–3T** with a longer Ni–Ni distance of 2.536 Å, lies 12.5 kcal mol^{-1} above **1N–Ni–1S**. The root-mean-square deviation (RMSD) was predicted to be 0.348 Å between the singlet **1N–Ni–2S** and the triplet **1N–Ni–3T**.

The singlet structure **1N–Ni–4S**, lying 14.0 kcal mol^{-1} in energy above **1N–Ni–1S**, has a six-electron donor bridging nickelallyllic ligand formed by double hydrogen migration bonded to the central Ni_2 unit similar to the manganallyllic ligand found in the experimentally known $(MeC_2NEt_2)Mn_2(CO)_7$ complex.[19] In **1N–Ni–4S** the nickelallyllic ligand is bonded to one CpNi unit as a trihapto ligand forming three Ni–C bonds and to the other CpNi unit by forming one dative N→Ni bond and one Ni–C bond. This configuration of bonds gives each nickel atom the favored 18-electron configuration without the need for a Ni–Ni bond. This is consistent with the relatively long Ni⋯Ni non-bonding distance of 2.888 Å in **1N–Ni–4S** suggesting the lack of a direct nickel–nickel bond.

Structures with hydrogen migration in the cobalt system $Cp_2Co_2(MeC_2NMe_2)$ are predicted to have significantly lower energies than either the tetrahedrane or dichotomy isomers.

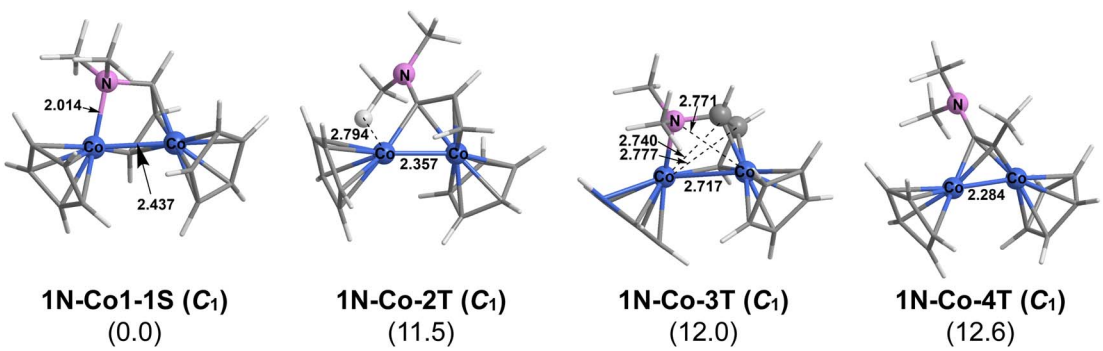

Fig. 10 The optimized low-energy $Cp_2Co_2(MeC_2NMe_2)$ structures. The symmetry of the structure is indicated in parentheses in the first line. The numbers in parentheses in the second line are the relative energies (ΔE in kcal mol^{-1}) predicted by M06-L/def2-TZVP method.

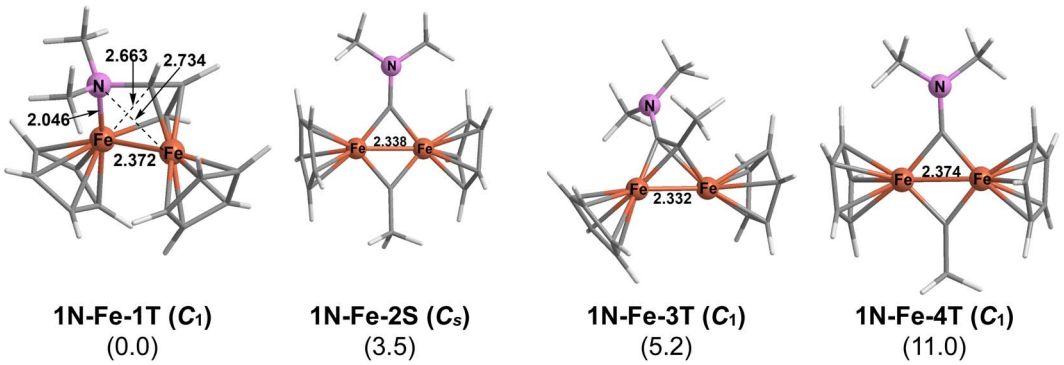

Fig. 11 The optimized low-energy $Cp_2Fe_2(MeC_2NMe_2)$ structures. The symmetry of the structure is indicated in parentheses in the first line. The numbers in parentheses in the second line are the relative energies (ΔE in kcal mol^{-1}) predicted by M06-L/def2-TZVP method.

Thus the lowest energy $Cp_2Co_2(MeC_2NMe_2)$ structure **1N–Co–1S** has a six-electron donor bridging cobaltallylic ligand bonded to the central Co_2 unit similar to the nickelallylic ligand in **1N–Ni–4S** or the manganallylic ligand in the experimentally known[19] $(MeC_2NEt_2)Mn_2(CO)_7$ complex (Fig. 10). The Co–Co distance of 2.437 Å in **1N–Co–1S** is clearly a bonding distance corresponding to the formal single bond that is required to give each cobalt atom the favored 18-electron configuration. This contrasts with **1N–Ni–4S** having the same type of metalallyllic ligand but with the much longer Ni⋯Ni distance of 2.888 Å where no nickel–nickel bond is needed to give each nickel atom the favored 18-electron configuration.

The next lower energy $Cp_2Co_2(MeC_2NMe_2)$ structure is the triplet **1N–Co–2T**, lying 11.5 kcal mol^{-1} above **1N–Co–1S** (Fig. 10). Structure **1N–Co–2T** has a bridging vinylcarbene ligand similar to that in **1N–Ni–2S** with a similar metal–metal bonding distance of 2.357 Å. However, since cobalt has one less electron than nickel, each cobalt atom in **1N–Co–2T** has only a 17-electron configuration consistent with its triplet spin state. The next $Cp_2Co_2(MeC_2NMe_2)$ structure **1N–Co–3T**, lying 12.0 kcal mol^{-1} in energy above **1N–Co–1S**, is a triplet version of **1N–Co–1S**. The Co–Co distance of 2.717 Å in **1N–Co–3T** is ~0.3 Å longer than that of 2.437 Å in **1N–Co–1S** implying the lack of a significant Co⋯Co interaction similar to the situation in **1N–Ni–4S**. The root-mean-square deviation (RMSD) was predicted to be 0.254 Å between the singlet **1N–Co–1S** and the triplet **1N–Co–3T**.

The lowest energy $Cp_2Co_2(MeC_2NMe_2)$ structure with an intact alkyne ligand without hydrogen migration and thus with a central Co_2C_2 tetrahedron, namely **1N–Co–4T** at 12.6 kcal mol^{-1} above **1N–Co–1S**, is also a triplet state structure. The Co–Co distance of 2.284 Å in **1N–Co–4T** is essentially

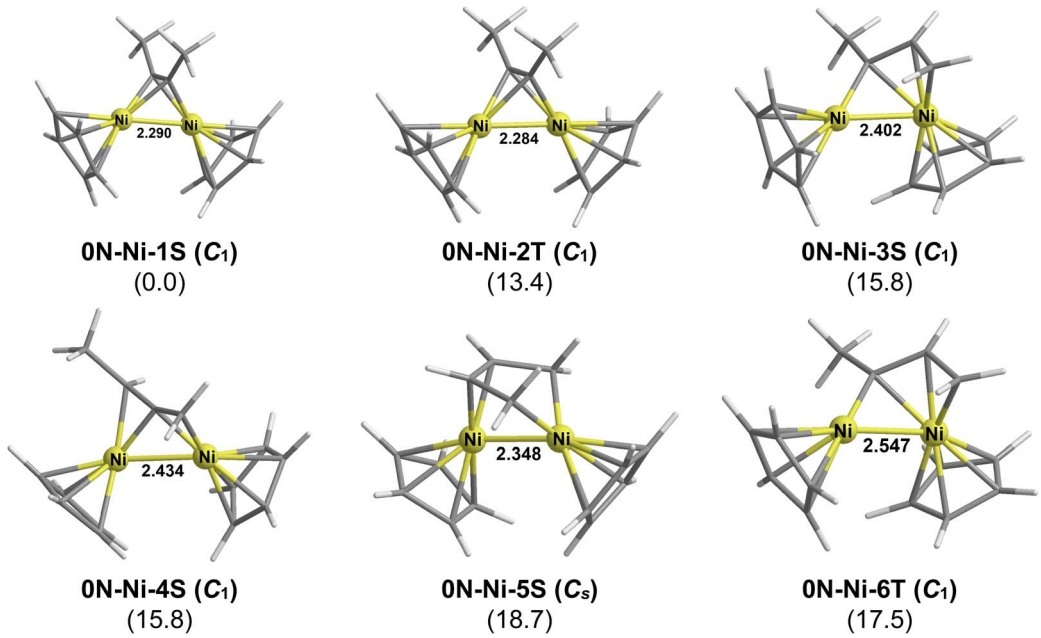

Fig. 12 The optimized low-energy $Cp_2Ni_2C_2Me_2$ structures. The symmetry of the structure is indicated in parentheses in the first line. The numbers in parentheses in the second line are the relative energies (ΔE in kcal mol^{-1}) predicted by M06-L/def2-TZVP method.

identical to the Ni–Ni distance of 2.293 Å in **1N–Ni–1S**. However, the WBI value of 0.84 for **1N–Co–4T** is larger than that of 0.72 for **1N–Ni–1S**, suggesting a σ + 2/2π type double bond. This gives each cobalt atom in **1N–Co–4T** an 18-electron configuration consistent with its triplet spin state.

The lowest energy $Cp_2Fe_2(MeC_2NMe_2)$ structure is a triplet structure **1N–Fe–1T** with a six-electron donor bridging ferrallylic ligand similar to **1N–Co–3T** (Fig. 10) and **1N–Ni–4S** (Fig. 9). The WBI value for the Fe–Fe distance of 2.372 Å in **1N–Fe–1T** is 0.92, which is much larger than that of 0.62 in **1N–Co–1S**, suggesting a σ + 2/2π type double bond. This gives each iron atom in **1N–Fe–1T** an 18-electron configuration consistent with its triplet spin state.

Hydrogen migration does not play a role in the next three $Cp_2Fe_2(MeC_2NMe_2)$ structures in terms of relative energies (Fig. 11). Structures **1N–Fe–2S** and **1N–Fe–4T**, lying 3.5 kcal mol^{-1} and 11.0 kcal mol^{-1} in energy, respectively, above **1N–Fe–1T**, are alkyne dichotomy structures completely analogous to the lowest energy $Cp_2Fe_2C_2(NMe_2)_2$ structures **2N–Fe–1S** and **2N–Fe–2T** with very similar Fe=Fe double bond distances. The root-mean-square deviation (RMSD) was predicted to be 0.104 Å between the singlet **1N–Fe–2S** and the triplet **1N–Fe–4T**. Structure **1N–Fe–3T**, lying 5.2 kcal mol^{-1} above **1N–Fe–1T** in energy, is a triplet tetrahedrane structure. Interpreting the Fe=Fe distance of 2.332 Å as a formal double bond gives each iron atom the 17-electron configuration for a binuclear triplet.

3.1.3 $Cp_2M_2C_2Me_2$. The potential energy surfaces become even more complicated for dimethylacetylene complexes of the type $Cp_2M_2C_2Me_2$ in which there are two methyl groups as sources of hydrogen atoms for migration to alkyne carbon atoms. Migrations of one hydrogen atom from each methyl group in a $Cp_2M_2C_2Me_2$ complex to an alkyne carbon atom can generate a bridging butadiene ligand (CH_2=CH–CH=CH_2) in which the methyl carbon atoms in the MeC≡CMe ligand become terminal carbon atoms and the alkyne carbon atoms

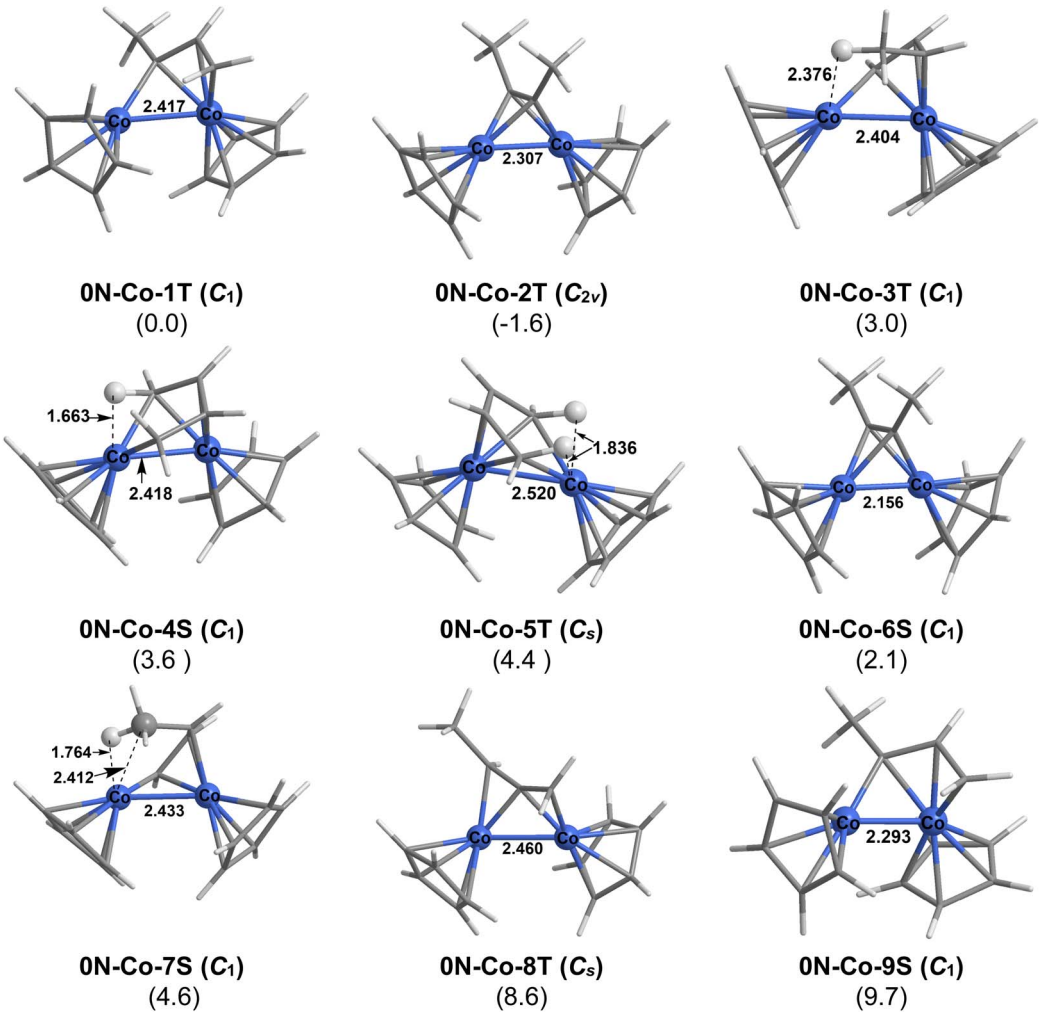

Fig. 13 The optimized low-energy $Cp_2Co_2C_2Me_2$ structures. The symmetry of the structure is indicated in parentheses in the first line. The numbers in parentheses in the second line are the relative energies (Δ*E* in kcal mol^{-1}) predicted by M06-L/def2-TZVP method. Four of the other seven low-energy $Cp_2Fe_2C_2Me_2$ structures, namely **0N–Fe–3T**, **0N–Fe–4T**, **0N–Fe–7S**, and **0N–Fe–8S**, have bridging ferrallylic ligands with the three higher energy structures clearly having agostic hydrogen C–H–Fe interactions. A bridging butadiene unit with one agostic C–H–Fe interaction is found in **0N–Fe–6T** and a bridging methylallene ligand is found in **0N–Fe–10T**.

become internal carbon atoms (d in Fig. 8). Such a bridging butadiene ligand consists of a metallacyclopentadiene (metallole) ring forming a tetrahapto bond to the other metal atom. In addition, one of the terminal hydrogens of the butadiene unit has an agostic C–H–M interaction with the ring metal atom. The overall structures of the $Cp_2M_2(CH_2{=}CH{-}CH{=}CH_2)$ bridging butadiene complexes arising from hydrogen migration from each methyl group of dimethylacetylene resemble that of the experimentally known[36] cobaltacyclopentadiene complex $Cp_2Co_2(\eta^4,\eta^2\text{-}C_4H_4)$ with the added feature of the agostic C–H–M interaction. In addition to the bridging butadiene complexes hydrogen migrations from one of the methyl groups in the MeC≡CMe ligand can lead to the same types of bridging allene, metalallylic, and vinylcarbene ligands found in the $Cp_2M_2(MeC_2NMe_2)$ complexes discussed above.

The nickel system is the only one of the three $Cp_2M_2C_2Me_2$ (M = Ni, Co, Fe) systems that has a reasonably simple potential energy surface (Fig. 12). The lowest energy $Cp_2Ni_2C_2Me_2$ structure by more than 13 kcal mol^{-1} (M06-L) is the alkyne complex **0N–Ni–1S** with a central Ni_2C_2 tetrahedrane unit similar to numerous experimentally known Cp_2Ni_2(alkyne) complexes.[15–17] The next $Cp_2Ni_2C_2Me_2$ isomer in terms of relative energy, namely **0N–Ni–2T**, can be regarded as the triplet excited state of **0N–Ni–1S** with similar geometry. The next three structures in terms of energy, namely the singlet structures **0N–Ni–3S**, **0N–Ni–4S**, and **0N–Ni–5S** lying 15.8, 15.8, and 18.7 kcal mol^{-1}, respectively, above **0N–Ni–1S** have bridging vinylcarbene, methylallene, and butadiene units, respectively. The butadiene derivative **0N–Ni–5S** does not have an agostic C–H–Ni interaction since a four-electron donor butadiene ligand without any such agostic interactions is sufficient to give each nickel atom the favored 18-electron configuration in a structure with an Ni–Ni single bond. Structure **0N–Ni–6T**, lying 17.5 kcal mol^{-1} above **0N–Ni–1S** in energy, is a triplet version of the singlet structure **0N–Ni–3S** with fundamentally the same geometry. The Ni–Ni distance of 2.547 Å in the triplet **0N–Ni–6T** is significantly longer than the Ni–Ni distance of 2.402 Å in the singlet **0N–Ni–3S**.

The potential energy surface becomes much more complicated for the cobalt system $Cp_2Co_2C_2Me_2$ with nine structures lying within 10 kcal mol^{-1} of the lowest energy structure (Fig. 13). The unchanged dimethylacetylene ligand without any hydrogen migration is found in the triplet structure **0N–Co–2T** of relatively high C_{2v} symmetry lying only 1.6 kcal mol^{-1} below

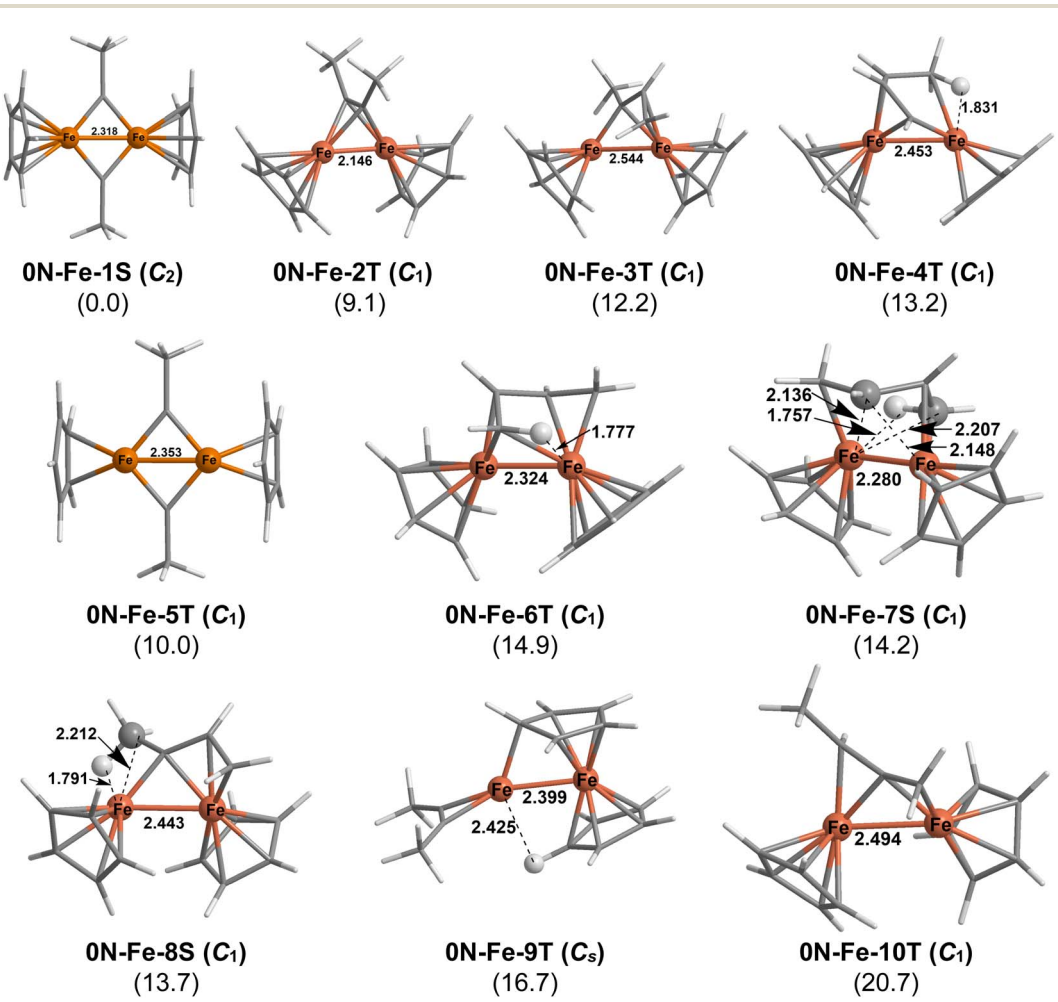

Fig. 14 The optimized low-energy $Cp_2Fe_2C_2Me_2$ structures. The symmetry of the structure is indicated in parentheses in the first line. The numbers in parentheses in the second line are the relative energies (ΔE in kcal mol^{-1}) predicted by M06-L/def2-TZVP method.

the global minimum as well in the higher energy singlet structure **0N–Co–6S**. Structures having central cobaltallylic units in various geometries and spin states are most prevalent being found in the lowest energy $Cp_2Co_2C_2Me_2$ structure **0N–Co–1T** as well as the triplet structure **0N–Co–3T** and the singlet structures **0N–Co–7S** and **0N–Co–9S**. The singlet structure **0N–Co–4S** and the triplet structure **0N–Co–5T** both have bridging butadiene ligands with one agostic C–H–Co interaction. A bridging methylallene ligand is found in structure **0N–Co–8T**.

The potential energy surface for the iron system $Cp_2Fe_2C_2Me_2$ is nearly as complicated as that of the corresponding cobalt system with ten structures lying within 22 kcal mol^{-1} of the lowest energy structure (Fig. 14). The lowest energy $Cp_2Fe_2C_2Me_2$ structure is the singlet structure **0N–Fe–1S** with two bridging three-electron donor methylcarbyne groups arising from dichotomy of the C≡C triple bond in dimethylacetylene. Structure **0N–Fe–1S** appears to be a particularly favorable structure since it lies more than 9 kcal mol^{-1} in energy below the next lowest energy structure. Interpreting the Fe═Fe distance of 2.318 Å in **0N–Fe–1S** as a formal double bond gives each iron atom the favored 18-electron configuration. The corresponding triplet alkyne dichotomy structure **0N–Fe–5T** with essentially the same Fe═Fe distance of 2.353 Å lies 12.8 kcal mol^{-1} above **0N–Fe–1S**. In **0N–Fe–5T** the triplet spin state arises from an Fe═Fe double bond of the $\sigma + 2/2\pi$ type similar to that in dioxygen as well as the triplet spin state organometallic derivative $(\eta^5\text{-}Me_5C_5)_2Fe_2(\mu\text{-}CO)_3$, that has been structurally characterized by X-ray crystallography.[35] The root-mean-square deviation (RMSD) was predicted to be 0.079 Å between the singlet **0N–Fe–1S** and the triplet **0N–Fe–5T**.

The second lowest energy $Cp_2Fe_2C_2Me_2$ structure, namely the triplet **0N–Fe–2T** lying 10.6 kcal mol^{-1} above **0N–Fe–1S**, has an intact dimethylacetylene ligand. Interpreting the Fe≡Fe distance (WBI = 1.24 in Table 1) of 2.150 Å as a triple $\sigma + \pi + \delta$ type bond gives each iron atom a 18-electron configuration for a binuclear triplet.

The remaining low-energy $Cp_2Fe_2C_2Me_2$ structure, namely the triplet **0N–Fe–9T** lying 16.6 kcal mol^{-1} above **0N–Fe–1S**, is the only Cp_2M_2(alkyne) isomer found in this work in which a cyclopentadienyl ring has migrated from one iron atom to the other (Fig. 14). This Cp migration results in one iron atom approaching a ferrocene-like environment by being bonded to a quasiterminal pentahapto η^5-Cp ligand and to four carbon atoms of a bridging η^4,η^1-Cp ligand. This sandwich-type ligand arrangement coupled with an Fe═Fe double bond of length 2.399 Å gives this central iron atom the favored 18-electron configuration provided that it bears a formal positive charge. The other iron atom in **0N–Fe–9T**, which is bonded to one carbon atom of the bridging η^4,η^1-Cp ligand, has a C–H–Fe agostic interaction with a C–H unit of the quasiterminal Cp ring, and bears an intact terminal MeC≡CMe ligand functioning as a four-electron donor through both π systems. This set of ligands combined with the Fe═Fe double bond gives this iron atom a 16-electron configuration provided that it bears a formal negative charge to balance the formal positive charge on the other iron atom. The 16-electron configuration of the iron bearing the alkyne ligand can account for the triplet spin state of **0N–Fe–9T**.

Table 1 Wiberg bond indices (WBIs) and Mayer bond indices (MBI) of the reported structures predicted by the M06-L/def2-TZPV method

Structure	Ni–Ni (Å)	WBI	MBI	Bond order
2N–Ni–1S	2.310	0.71	0.68	1
2N–Ni–2T	2.359	0.62	0.55	1
2N–Ni–3S	3.496	0.22	0.16	0
2N–Ni–4S	2.790	0.32	0.19	0
2N–Co–1S	2.360	0.71	0.54	1
2N–Co–2T	2.314	0.82	0.81	2
2N–Co–3S	2.236	0.85	0.87	2
2N–Co–4S	2.624	0.54	0.47	1
2N–Co–5T	2.556	0.63	0.42	1
2N–Fe–1S	2.344	0.85	0.77	2
2N–Fe–2T	2.360	0.86	0.72	2
2N–Fe–3S	2.278	1.14	1.21	3
2N–Fe–4T	2.555	0.61	0.54	1
2N–Fe–5S	2.468	0.71	0.70	2
1N–Ni–1S	2.300	0.72	0.71	1
1N–Ni–2S	2.379	0.56	0.52	1
1N–Ni–3T	2.531	0.45	0.38	1
1N–Ni–4S	2.903	0.26	0.15	0
1N–Co–1S	2.436	0.62	0.52	1
1N–Co–2T	2.356	0.64	0.61	1
1N–Co–3T	2.714	0.37	0.26	1
1N–Co–4T	2.302	0.82	0.79	1
1N–Fe–1T	2.370	0.92	0.86	2
1N–Fe–2S	2.345	0.81	0.68	2
1N–Fe–3T	2.345	0.87	0.83	2
1N–Fe–4T	2.381	0.79	0.61	2
0N–Ni–1S	2.294	0.72	0.73	1
0N–Ni–2T	2.285	0.71	0.67	1
0N–Ni–3S	2.400	0.53	0.49	1
0N–Ni–4S	2.432	0.53	0.55	1
0N–Ni–5S	2.342	0.58	0.55	1
0N–Ni–6T	2.545	0.44	0.38	1
0N–Co–1T	2.417	0.63	0.59	1
0N–Co–2T	2.312	0.84	0.84	2
0N–Co–3T	2.404	0.61	0.59	1
0N–Co–4S	2.416	0.65	0.60	1
0N–Co–5T	2.524	0.51	0.37	1
0N–Co–6S	2.159	1.05	1.12	2
0N–Co–7S	2.432	0.61	0.57	1
0N–Co–8T	2.454	0.60	0.59	1
0N–Co–9S	2.291	0.85	0.83	2
0N–Fe–1S	2.326	0.79	0.56	2
0N–Fe–2T	2.150	1.24	1.38	3
0N–Fe–3T	2.542	0.64	0.60	2
0N–Fe–4T	2.450	0.72	0.65	2
0N–Fe–5T	2.338	0.80	0.56	2
0N–Fe–6T	2.330	0.87	0.81	2
0N–Fe–7S	2.280	0.87	0.80	2
0N–Fe–8S	2.437	0.71	0.68	2
0N–Fe–9T	2.398	0.57	0.58	1
0N–Fe–10T	2.490	0.66	0.63	1

3.2 Wiberg bond indices

The Wiberg Bond Indices and Mayer Bond Indices of the binuclear cyclopentadienylmetal alkyne systems $Cp_2M_2C_2R_2$ (M = Ni, Co, Fe; R = Me and NMe_2) have been investigated by

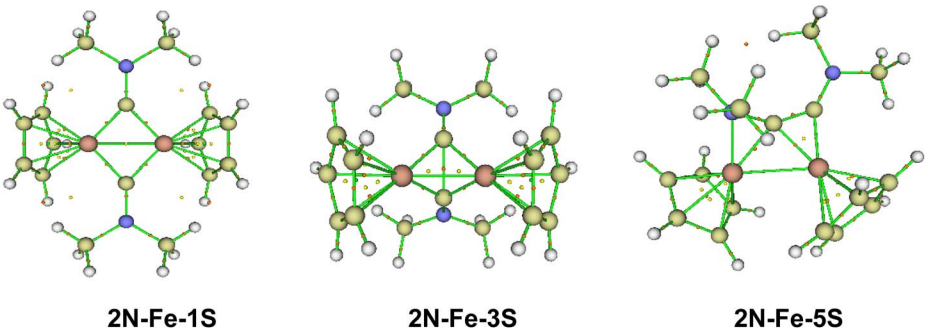

Fig. 15 QTAIM analysis of the singlet $Cp_2Fe_2C_2(NMe_2)_2$ structures.

using the MultiWFN software (Table 1).[37] They are comparable to each other; only the Wiberg Bond Indices (WBIs) are reported in the text. The Wiberg Bond Indices (WBIs) for metal–metal bonds involving transition metal atoms do not match the conventional chemical bond order assumptions, but instead are much smaller than such conventional formal bond orders. However, the relative WBI values for transition metal M–M bonds provide insight regarding the corresponding formal metal–metal bond orders. For the present systems, the WBIs range from 0.37 to 0.84 for M–M single bonds, from 0.71 to 0.92 for M=M double bonds, and from 1.14 to 1.24 for M≡M triple bonds.

Taking the singlet $Cp_2Fe_2C_2(NMe_2)_2$ structures as examples, the Bond Critical Points (BCPs), Ring Critical Points (RCPs), and Cage Critical Points (CCPs) have been plotted by using the MultiWFN software (Fig. 15). However, no obvious BCPs between the two iron atoms or between the nitrogen atom and the iron atom were observed. This suggests that there is no pure metal–metal bonding or nitrogen–metal bonding. Instead, multicenter bond characters (RCP and CCP) are displayed in these structures. However, use of the formal metal–metal bond orders suggested by the WBI data (Table 1) leads to reasonable electron bookkeeping for these molecules.

3.3 A hydrogen migration mechanism

A possible double hydrogen migration scheme starting with the $Cp_2Co_2(MeC_2NMe_2)$ complex to give the cobaltallylic complex $Cp_2Co_2(C_3H_3NMe_2)$ is depicted in Fig. 16. Five transition states

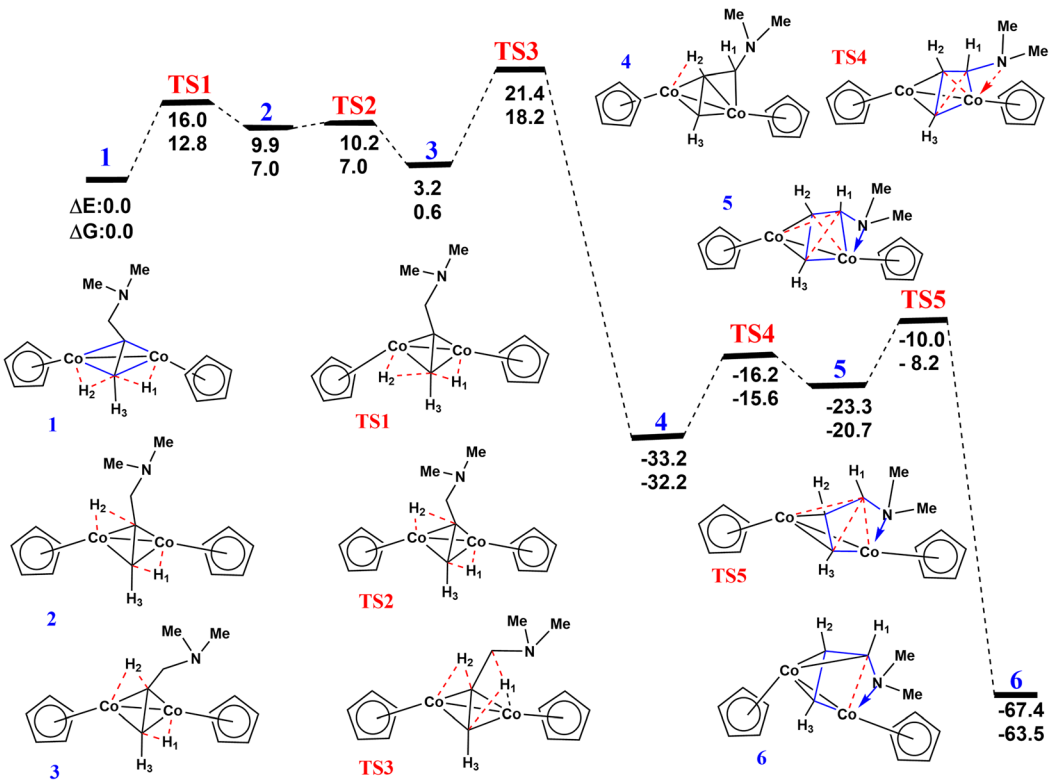

Fig. 16 Proposed hydrogen migration path for the $Cp_2Co_2(MeC_2NMe_2)$ system predicted by the M06-L/def2-TZVP method.

have been identified. The initial complex **1** with two agostic C–H–Co interactions can be formed when the free $MeC{\equiv}CNMe_2$ ligand reacts with a suitable CpCo source. Transfer of the hydrogen atom H_2 in **1** from the γ-C to the β-C through transition state TS-1 can then occur with an activation energy barrier of $\Delta G = 12.8$ kcal mol^{-1} to give **2**. The other hydrogen atom H_1 can then migrate from the γ-C to the α-C through transition states TS-2 and TS-3 with a activation energy barrier of $\Delta G = 18.2$ kcal mol^{-1} to form **4** that retains the agostic C–H_2–Co interaction. In **4**, the C_3H_3 unit is bonded to one cobalt atom as a trihapto ligand using all three carbon atoms whereas only the β-C and γ-C atoms are bonded to the other cobalt atom. The Me_2N unit then attacks one cobalt atom in **4** through transition state TS-4 with an activation energy barrier ΔG of 15.6 kcal mol^{-1} to displace the agostic hydrogen atom thereby giving **5** with no changes in the bonding of the hydrocarbon part of the $Me_2NC_3H_3$ ligand. Finally, migration of a carbon atom from the cobalt atom bonded to three carbon atoms in **5** to the other cobalt atom through transition state TS-5 with an activation energy barrier ΔG of 8.2 kcal mol^{-1} gives the cobaltallylic derivative **6** corresponding to the lowest energy $Cp_2Co_2(MeC_2NMe_2)$ isomer **1N–Co–1S** in Fig. 10. The coordination mode of the bridging $Me_2NC_3H_3$ cobaltallylic ligand in **6** is similar to that of the bridging $Et_2NC_3H_3$ manganallylic ligand in the experimentally known and structurally characterized complex $Mn_2(CO)_7(C_3H_3NMe_2)$.[19]

4. Conclusion

The $Cp_2M_2C_2(NMe_2)_2$ (M = Ni, Co, Fe) systems have the simplest potential energy surfaces of the Cp_2M_2(alkyne) systems studied in this work. Thus the low-energy structures in these systems are limited to tetrahedrane complexes with an intact alkyne ligand and a central M_2C_2 tetrahedron and the alkyne dichotomy products $Cp_2M_2(CNMe_2)_2$ in which the C≡C triple bond of the original alkyne is completely broken to give two separate bridging dimethylaminocarbyne ligands. The relative energies of these two structure types depend on the electron requirements of the central metal atoms. Thus for the nickel system $Cp_2Ni_2C_2(NMe_2)_2$ the tetrahedrane complex, corresponding to extensive series of known Cp_2Ni_2(alkyne) complexes[15–17] and having favorable 18-electron nickel configurations, is favored energetically by a substantial margin greater than 23 kcal mol^{-1}. For the cobalt system $Cp_2Co_2C_2(NMe_2)_2$ the singlet and triplet tetrahedrane structures and a singlet dichotomy structure have similar energies within ~3 kcal mol^{-1}. For the iron system $Cp_2Fe_2C_2(NMe_2)_2$ both singlet and triplet dichotomy structures lie more than 12 kcal mol^{-1} in energy below the lowest energy structures with intact alkyne ligands. Furthermore, the intact alkyne ligands in the complexes $Cp_2Fe_2(Me_2NC_2NMe_2)$ are six-electron donors to the central Fe_2 unit by forming an N→Fe dative bond from one of the Me_2N substituents in addition to the usual π-bonds to iron atoms from both of the π-components in the alkyne C≡C triple bond.

The Cp_2M_2(alkyne) systems based on the alkynes $MeC{\equiv}CNMe_2$ and MeC≡CMe, have methyl groups directly linked to alkyne carbon atoms. This makes their hydrogen atoms more accessible for migration to alkyne carbon atoms than the more remotely located methyl hydrogen atoms on the amino nitrogen atoms in the $Cp_2M_2(Me_2NC{\equiv}CNMe_2)$ systems. Therefore, the potential energy surfaces of the $MeC{\equiv}CNMe_2$ and MeC≡CMe systems are complicated. However, for the nickel systems $Cp_2Ni_2(MeC_2NMe_2)$ and $Cp_2Ni_2C_2Me_2$ with enough d electrons from the nickel atoms, it is not necessary to completely cleave the C≡C bond for the nickel atoms to have the favored 18-electron configuration. Therefore the tetrahedrane complexes with intact alkyne ligands remain the lowest energy structures again corresponding to several experimentally known Cp_2Ni_2(alkyne) complexes.[15,16] However, for the cobalt and iron systems derived from the $MeC{\equiv}CNMe_2$ ligand, the singlet and triplet metalallylic structures $Cp_2M_2(CHCHCHNMe_2)$ arising from migration of two methyl hydrogen atoms, one to each alkyne carbon atom, are the lowest energy structures. This situation is similar to that in the experimentally known manganese carbonyl complexes $(Et_2NC_2Me)Mn_2(CO)_8$ of alkynes with methyl substituents where hydrogen migration from the methyl group to one or both alkyne carbon atoms is observed to give species with bridging allene or manganallyl units (Fig. 2).[19] For the cobalt system derived from dimethylacetylene, the $Cp_2Co_2(CH_2CHCMe)$ vinylcarbene structure with migration of one methyl hydrogen atom to the adjacent alkyne carbon atom is the lowest energy structure. For the iron system derived from dimethylacetylene, the alkyne dichotomy $Cp_2Fe_2(CMe)_2$ structure is the lowest energy structure.

The sets of low-energy $Cp_2M_2(MeC_2NMe_2)$ and $Cp_2M_2C_2Me_2$ isomers formed by hydrogen migration processes also include structures with bridging allene ligands and with bridging vinylcarbene ligands formed by migration of a single methyl hydrogen to the remote alkyne carbon atom (the γ-carbon atom) and to the adjacent alkyne carbon atom (the β-carbon atom), respectively. In addition, the set of low-energy structures for the $Cp_2M_2C_2Me_2$ (M = Co, Fe) systems derived from dimethylacetylene includes derivatives with bridging butadiene ligands formed by migration of one hydrogen atom from each methyl group to an alkyne carbon atom.

Five transition states have been identified in a possible mechanistic sequence for double hydrogen migration in the $Cp_2Co_2/MeC{\equiv}CNMe_2$ system to give the cobaltallylic complex $Cp_2Co_2(C_3H_3NMe_2)$ found to be the lowest energy structure of $Cp_2Co_2(MeC_2NMe_2)$ stoichiometry. This mechanistic sequence has intermediates with C–H–Co interactions through agostic hydrogen atoms and successive activation energy barriers of 13.1, 17.0, 15.2, and 12.0 kcal mol^{-1}.

Data availability

Data are presented in the ESI† and are available from Prof. Huidong Li.

Conflicts of interest

The authors declare no competing financial interests.

Acknowledgements

The research in Chengdu was supported by the Sichuan Provincial Foundation for Distinguished Young Leaders of Disciplines in Science and Technology of China (Grant-Nos.2019JDJQ0051 and 2019JDJQ0050), the Chunhui Program of the Ministry of Education of China (Grant Z2017091), and the Open Research Subject of the Key Laboratory of Advanced Computation in Xihua University (Grant No. szjj2017-011 and szjj2017-012). The research at the University of Georgia was supported by the U. S. Department of Energy, Basic Energy Sciences, Division of Chemistry, Computational and Theoretical Chemistry (CTC) Program under Contract DE-SC0018412.

References

1 H. Greenfield, H. W. Sternberg, R. A. Friedel, J. H. Wotiz, R. Markby and I. Wender, Acetylenic dicobalt hexacarbonyls—organometallic compounds derived from alkynes and dicobalt octacarbonyl, *J. Am. Chem. Soc.*, 1956, **78**, 120–124.

2 R. S. Dickson and P. J. Fraser, Compounds derived from alkynes and carbonyl complexes of cobalt, *Adv. Organomet. Chem.*, 1974, **12**, 323–377.

3 M. J. Went, Synthesis and reactions of polynuclear cobalt alkyne complexes, *Adv. Organomet. Chem.*, 1997, **41**, 69–125.

4 S. E. Gibson and N. Mainolfi, The intermolecular Pauson–Khand reaction, *Angew. Chem., Int. Ed.*, 2005, **44**, 3022–3037.

5 K. M. Nicholas, Chemistry and synthetic utility of cobalt-complexed propargyl cations, *Acc. Chem. Res.*, 1987, **20**, 207–214.

6 N. Iwasawa, I. Ooi and K. Inaba, [4+2] Cycloaddition reaction of cyclic alkyne-$\{Co_2(CO)_6\}$ complexes with dienes, *Angew. Chem., Int. Ed.*, 2010, **49**(41), 7534–7537.

7 I. Ooi, T. Sakurai and J. Takaya, Protonation-triggered generation of acylcobalt species from alkyne-$[Co_2(CO)_6]$ complexes and their reaction with alkenes, *Chem. Eur J.*, 2012, **18**, 14618–14621.

8 N. A. Danilkina, A. G. Lyapunova and A. F. Khlebnikov, Ring-closing metathesis of $Co_2(CO)_6$-alkyne complexes for the synthesis of 11-membered dienediynes: overcoming thermodynamic barriers, *J. Org. Chem.*, 2015, **80**, 5546–5555.

9 B. Alcaide, C. Polanco and M. A. Sierra, Alkyne-$Co_2(CO)_6$ complexes in the synthesis of fused tricyclic beta-lactam and azetidine systems, *J. Org. Chem.*, 1998, **63**, 6786–6796.

10 W. Hübel, in *Organic Syntheses via Metal Carbonyls*, ed. I. Wender and P. Pino, Interscience—Wiley, New York, vol. 1, 1968, pp. 273–342.

11 F. A. Cotton, J. D. Jamerson and B. R. Stults, Metal-metal multiple bonds in organometallic compounds. 1. (Di-tert-butylacetylene)hexacarbonyldiiron and hexacarbonyldicobalt, *J. Am. Chem. Soc.*, 1976, **98**, 1774–1779.

12 R. B. King and C. A. Harmon, Novel products from reactions of aminoalkynes with metal carbonyls, *Inorg. Chem.*, 1976, **15**, 879–885.

13 G. G. Cash, R. C. Pettersen and R. B. King, X-ray crystal and molecular structure of $[Et_2NCFe(CO)_3]_2$—example of division of an alkyne into 2 separate units by rupture of the C≡C bond, *Chem. Commun.*, 1977, 30–31.

14 H. Li, H. Feng, W. Sun, Y. Xie, R. B. King and H. F. Schaefer, Alkyne dichotomy: splitting of bis(dialkylamino)acetylenes, dimethoxyacetylene, bis(methylthio)acetylene, and their heavier congeners to give carbyne ligands in iron carbonyl derivatives, *Organometallics*, 2013, **32**, 88–94.

15 J. F. Tilney-Bassett and O. Mills, Cyclopentadienylnickel-acetylene complexes, *J. Am. Chem. Soc.*, 1959, **81**, 4757–4758.

16 J. F. Tilney-Bassett, Cyclopentadienylnickel-acetylene complexes, *J. Chem. Soc.*, 1961, 577–581.

17 E. J. Forbes and N. Iranpoor, Dicyclopentadienylnickel alkyne complexes: photochemical formation and mass spectra, *J. Organomet. Chem.*, 1982, **236**, 403–407.

18 D. Kumar, M. Deb, J. Singh, N. Singh, K. Keshav and A. J. Elias, Chemistry of the highly stable hindered cobalt sandwich compound $(\eta^5\text{-Cp})Co(\eta^4\text{-}C_4Ph_4)$ and its derivatives, *Coord. Chem. Rev.*, 2016, **306**, 115–170.

19 R. D. Adams, G. Chen and Y. Chi, Coordination and transformations of the ynamine ligand in a dimanganese complex, *Organometallics*, 1992, **11**, 1473–1479.

20 Y. Zhao and D. G. Truhlar, A new local density functional for main-group thermochemistry, transition metal bonding, thermochemical kinetics, and noncovalent interactions, *J. Chem. Phys.*, 2006, **12**, 194101–194107.

21 Y. Zhao and D. G. Truhlar, The M06 suite of density functionals for main group thermochemistry, thermochemical kinetics, noncovalent interactions, excited states, and transition elements: two new functionals and systematic testing of four M06-class functionals and 12 other functionals, *Theor. Chem. Acc.*, 2008, **120**, 215–241.

22 J. D. Chai and M. Head-Gordon, Long-range corrected hybrid density functionals with damped atom-atom dispersion corrections, *Phys. Chem. Chem. Phys.*, 2008, **10**, 6615–6620.

23 M. J. Frisch, *et al.*, *Gaussian 16, Revision C.01*, Gaussian, Inc., Wallingford CT, 2019.

24 (*a*) J. P. Perdew and Y. Wang, Accurate and simple analytic representation of the electron gas correlation energy, *Phys. Rev. B:Condens. Matter Mater. Phys.*, 1992, **45**, 13244–13249; (*b*) J. P. Perdew, K. Burke and Y. Wang, Generalized gradient approximation for the exchange-correlation hole of a many-electron system, *Phys. Rev. B:Condens. Matter Mater. Phys.*, 1996, **54**, 16533–16539.

25 (*a*) S. Grimme, Density functional theory with London dispersion corrections. Wires Comput, *Mol. Sci.*, 2011, **1**, 211–228; (*b*) M. Dierksen and S. Grimme, An efficient approach for the calculation of Franck-Condon integrals of large molecules, *J. Chem. Phys.*, 2005, **122**, 244101.

26 Y. Zhao and D. G. Truhlar, Density functionals with broad applicability in chemistry, *Acc. Chem. Res.*, 2008, **41**, 157–167.

27 T. H. Dunning Jr, Gaussian basis functions for use in molecular calculations. I. Contraction of (9s5p) atomic basis sets for the first-row atoms, *J. Chem. Phys.*, 1970, **53**, 2823–2833.

28 S. Huzinaga, Gaussian-type functions for polyatomic systems. I, *J. Chem. Phys.*, 1965, **42**, 1293–1302.
29 A. J. H. Wachters, Gaussian basis set for molecular wavefunctions containing third-row atoms, *J. Chem. Phys.*, 1970, **52**, 1033–1036.
30 D. M. Hood, R. M. Pitzer and H. F. Schaefer, Electronic structure of homoleptic transition metal hydrides: TiH_4, VH_4, CrH_4, MnH_4, FeH_4, CoH_4, and NiH_4, *J. Chem. Phys.*, 1979, **71**, 705–712.
31 F. Weigend and R. Ahlrichs, Balanced basis sets of split valence, triple zeta valence and quadruple zeta valence quality for H to Rn: Design and assessment of accuracy, *Phys. Chem. Chem. Phys.*, 2005, **7**, 3297–3305.
32 F. Weigend, Accurate Coulomb-fitting basis sets for H to Rn, *Phys. Chem. Chem. Phys.*, 2006, **8**, 1057–1065.
33 (*a*) Calculate Root-mean-square deviation (RMSD) of Two Molecules Using Rotation, *GitHub*, **http://github.com/charnley/rmsd**; (*b*) W. Kabsch, A solution for the best rotation to relate two sets of vectors, *Acta Crystallogr.*, 1976, **A32**, 922–923; (*c*) M. W. Walker, L. Shao and R. A. Volz, Estimating 3-D location parameters using dual number quaternions, *CVGIP: Image Understanding*, 1991, vol. 54, pp. 358–367.
34 O. S. Mills and B. W. Shaw, The structure of (diphenylacetylene)bis(cyclopentadienylnickel), *J. Organomet. Chem.*, 1968, **3**, 595–600.
35 J. P. Blaha, B. E. Bursten, J. C. Dewan, R. B. Frankel, C. L. Randolph, B. A. Wilson and M. S. Wrighton, Dinuclear, 18-electron species having a triplet ground state—isolation, characterization, and crystal structure of photogenerated $(\eta^5\text{-}C_5Me_5)_2Fe_2(\mu\text{-}CO)_3$, *J. Am. Chem. Soc.*, 1985, **107**, 4561–4562.
36 M. Rosenblum, B. North, D. Wells and W. P. Giering, Synthesis and chemistry of η^4-cyclobutadiene(η^5-cyclopentadienyl)cobalt, *J. Am. Chem. Soc.*, 1972, **94**, 1239–1245.
37 (*a*) T. Lu and F. M. Chen, A Multifunctional Wavefunction Analyzer, *J. Comput. Chem.*, 2012, **33**, 580–592; (*b*) T. Lu, A comprehensive electron wavefunction analysis toolbox for chemists, Multiwfn, *J. Chem. Phys.*, 2024, **161**, 082503.